

Determination of trigger delays for strain independent cardiac diffusion measurements based on automated segmentation of cine images

Peter Speier¹, Andreas Greiser¹, Christoph Guetter², and Marie-Pierre Jolly²

¹Siemens AG Healthcare Sector, Erlangen, Germany, ²Imaging and Computer Vision, Siemens Corporation, Corporate Technology, Princeton, NJ, United States

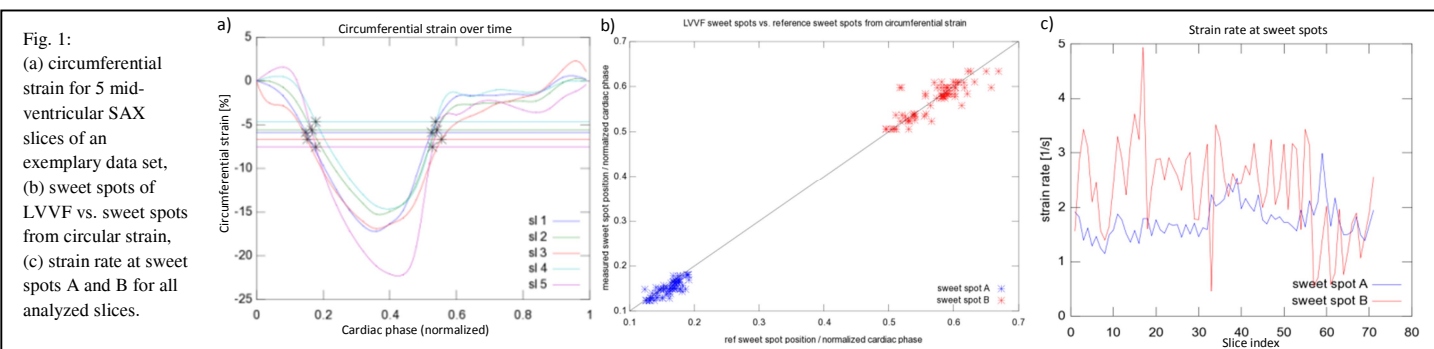
Introduction: Measurements of diffusion in the heart require special motion-insensitive acquisition methods. Double-triggered stimulated-echo preparation (DTST) eliminates heart motion by placing encoding and decoding gradients in the same phase of the cardiac cycle [1]. DTST with monopolar diffusion-encoding (DTST-MP) gradients has been shown to provide robust DTI data in patients [2]. Encoding takes place during a full cardiac cycle, therefore tissue deformation (strain) due to cardiac motion will deform the encoded pattern and thus affect the diffusion quantification [3]. DTST with bipolar diffusion encoding (DTST-BP) limits the encoding time to one cardiac phase, its results are thus independent of cardiac strain [4]. However, bipolar encoding requires longer echo times, which results in reduced SNR due to T2 decay in an already SNR-starved method, and leads to increased motion sensitivity in the readout (EPI) module, leaving DTST-MP as the most promising method for clinical work.

DTST-MP measurements are strain independent if the encoding and decoding takes place at time points of average strain in the encoding direction. In normal hearts, all left-ventricular (LV) strain components are highly correlated [5]; therefore (1) a single-strain component, e.g., radial, is representative for all, and (2), all strain components assume their average values at the same time. Under this condition there exist two "sweet spots" A and B in the cardiac cycle, one near the beginning of the contraction phase (A) and one near the end (B). For exact diffusion results, the positions of these sweet spots must be determined and the trigger delay of the diffusion measurement must be adapted. The cardiac strain time curve, and from it the sweet spots, can be determined from an additional strain-sensitive measurement, e.g., tissue-phase mapping [6], or a tagged Cine [7]. The goal of this work is to show that the sweet spot positions can be determined without the need for additional strain measurements and analysis, but from segmentation of clinical bSSFP cine images that are typically part of a cardiac exam anyway.

Methods: *Strain Reference:* Motion on Cine bSSFP images can be tracked and expressed as a deformation field [8]. Analog to the Vector Velocity Imaging (VVI) method in Ultrasound, we generated strain reference curves from these deformation fields using an internal prototype application [9]. We use the average circumferential strain component as strain reference because it can be determined with highest accuracy [10]. Sweet spots of average circumferential strain were determined as the time points where the time curves assume their time-averaged value.

LV Endo-Contour (EC) Segmentation: Automated algorithms exist for segmenting the LV myocardial borders on Cine bSSFP images [11]. The endocardial border can be determined very robustly and accurately due to the good contrast between blood pool and myocardium. In our implementation, the papillary muscles are assigned to the blood pool. The algorithm also detects the LV base plane (as defined by the mitral valve) and determines the LV volume time curve (LVVF) as one measure for LV deformation. Slice-independent sweet-spot positions were calculated from LVVF curves.

Data: 22 Cine bSSFP data sets were collected from 9 healthy volunteers on 1.5T and 3T scanners (Siemens AG, Erlangen) with various clinical parameter settings (9-12 SAX slices covering apex to LV atrium, approx. 40ms temporal resolution). Reference sweet-spot positions for radial and circumferential strain and sweet-spot positions derived from LVVF were calculated as described above. Because sweet-spot reference positions are very similar for mid-ventricular (MV) slices and vary for basal and apical SAX slices, analysis was limited to 2-4 MV slices in each data set (71 slices in total), selected based on the following criteria: (1) first MV slice: second slice from the valve plane, (2) last MV slice: third most apical slice.



Results: Figure 1a shows exemplary curves of circumferential strain for 5 MV SAX slices of one exam. Sweet-spot positions agree well for all slices. Fig 1b compares LVVF derived sweet-spot positions with reference sweet-spot positions. LVVF derived positions agree closely for both sweet spot A with $\Delta T(A) = (-10 \pm 11)$ ms, and B with $\Delta T(B) = (-2 \pm 22)$ ms. The relative error E in the diffusion results from incorrect placement of encoding gradients can be estimated as $E = 2 \cdot R(X) \cdot \Delta T(X)$ with $R(X)$ being the strain rate at position X and $\Delta T(X)$ being the time between encoding and position of sweet spot X. The slopes of the exemplary curves in Figs. 1a indicate that R is smaller for sweet spot A than for sweet spot B. Fig. 1c shows strain rates at the sweet spots for all analyzed slices; average values are $R(A) = (1.8 \pm 0.3) s^{-1}$, and $R(B) = (2.3 \pm 0.9) s^{-1}$. This suggests that, on average, diffusion results from DTST-MP measurements will be less affected by strain if encoded in sweet spot A instead of in sweet spot B.

Discussion and Conclusion: We have demonstrated that strain-free cardiac diffusion measurements of mid-ventricular SAX slices with the DTST-ME method can be planned without the need for additional strain measurements and evaluations. Instead, the correct trigger delay can be determined with a high degree of accuracy from clinical Cine bSSFP images using fully automated segmentation algorithms. To improve the accuracy of the method further, and to extend its validity to all apical and basal LV SAX slices, slice-specific measures derived from endocardial contours could be used instead of LV blood volume.

References: [1] Edelman RR, et al., Magn Reson Med. 1994, 32(3):423-8. [2] Laura-Ann McGill, et al., JCVMR 2012, 14:86. [3] Tseng WY, et al., Magn Reson Med. 1999, 42(2):393-403. [4] Dou J, et al., Magn Reson Med. 2002, 48(1):105-14. [5] Reese TG, et al., Magn Reson Med. 1995, 34(6):786-91. [6] Petersen SE, et al., Radiology 2006 238:3, 816-826 [7] Shehata ML, et al., JCVMR, 2009, 11:55 [8] Guetter C, et al, ISBI 2011, 590-593. [9] TrufiStrain, Siemens Corporation, Corporate Technology. [10] K Kalisz K et al, RSNA 2013, accepted scientific presentation [11] Jolly M.-P., et al, ISBI 2010, 484-487.